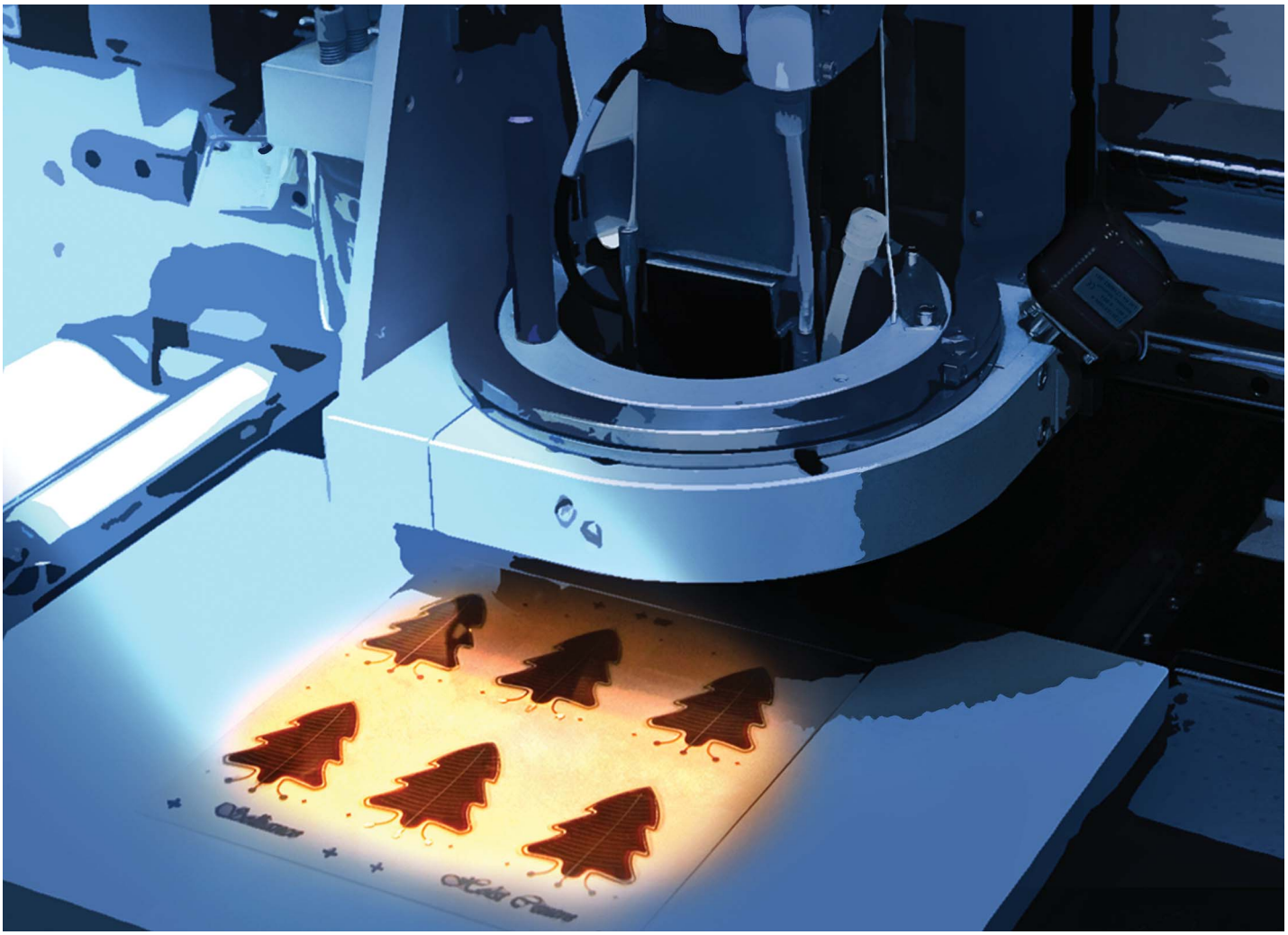

Showcasing the work on inkjet printing of organic solar cells presented by a group of scientists from Holst Centre, ECN and imec, united in Solliance alliance.

Title: High efficiency, fully inkjet printed organic solar cells with freedom of design

All-inkjet printed large area organic solar cells deposited from environmentally friendly solvents in an air atmosphere using industrial scale printheads are demonstrated for the first time.

As featured in:

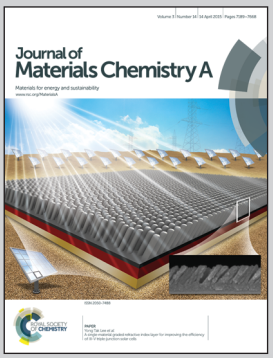

See Y. Galagan, W. A. Groen *et al.*, *J. Mater. Chem. A*, 2015, **3**, 7255.

ROYAL SOCIETY OF CHEMISTRY

www.rsc.org/MaterialsA

Registered charity number: 207890

Journal of Materials Chemistry A

PAPER

View Article Online
View Journal | View Issue

Cite this: J. Mater. Chem. A, 2015, 3, 7255

High efficiency, fully inkjet printed organic solar cells with freedom of design

T. M. Eggenhuisen,[a] Y. Galagan,*[b] A. F. K. V. Biezemans,[cd] T. M. W. L. Slaats,[a] W. P. Voorthuijzen,[b] S. Kommeren,[a] S. Shanmugam,[b] J. P. Teunissen,[a] A. Hadipour,[e] W. J. H. Verhees,[cd] S. C. Veenstra,[cd] M. J. J. Coenen,[a] J. Gilot,[b] R. Andriessen[b] and W. A. Groen*[ae]

Received 22nd January 2015
Accepted 11th February 2015

DOI: 10.1039/c5ta00540j

www.rsc.org/MaterialsA

The organic photovoltaics field is maturing and reaching a technology readiness level where the focus is on developing large scale fabrication methods. In this light, fully inkjet printed organic solar cells were demonstrated. Inkjet printing allows direct patterning of all the layers, including the electrodes, offering full freedom of design without the use of masks or structuring by hardware. The semitransparent front and back electrodes consist of PEDOT:PSS and conductive Ag fingers, avoiding the use of ITO. The inkjet printing of six functional layer demonstrated minimal losses in performance as compared to the lab-scale standard, spin coated devices. All-inkjet printed large area (>1 cm^2) organic solar cells with power conversion efficiency of 4.1% deposited from environmentally friendly solvents in an air atmosphere are demonstrated for the first time. Organic solar cells were fabricated using industrial scale (512 nozzles) printheads, compatible with R2R technology. To prove the great advantage of inkjet printing as a digital technology allowing freedom of forms and designs, large area organic solar cells with different artistic shapes were demonstrated. Reported results confirm that inkjet printing has high potential for the processing of OPV, allowing quick changes in design as well as the materials.

Introduction

Silicon photovoltaics are increasingly becoming part of the streetscape. Several emerging thin film technologies are also reaching a level of technology readiness such that industrial production, albeit on small scales, is starting up. For a competitive business case, the efficiency, cost and lifetime are critical parameters.[1] In the case of organic photovoltaics, small molecule tandem cells prepared by evaporation with 12% registered power conversion efficiency[2] and triple-junction polymer solar cells with 11.5% power conversion efficiency[3] lead the way. Solution processing by roll-to-roll (R2R) technology has been proposed as a means to produce organic photovoltaics at low cost and high through-put.[4–7] For this, various deposition techniques[7,8] have been combined to apply the photo-active layer and electrodes. Krebs *et al.* have demonstrated several times all-solution process organic solar cells by R2R printing and coating, using different cells architectures and materials.[9–11] Some successful examples of integration of the OPV into the final products were already demonstrated.[12–15] Nonetheless, there are still a few scientific and technological hurdles to be taken to achieve the needed combination of low cost and high efficiency modules to interest the industry and the consumer market. One of the remaining issues towards application and integration of OPV is the possibility to customize shape and dimensions of the modules. Slot die coating, which is widely used for the R2R manufacturing of OPV utilizes stripe patterning in one direction providing only rectangular shaped modules. R2R production technology, which can change the module design on the request of customers until now often involves a combination of different deposition techniques and post-process structuring, using *e.g.* laser ablation.[16,17] This requires a lot of investments into the equipment. Inkjet printing[18] is a deposition technique which has the main advantage that it is drop-on-demand: deposition patterns are simply changed through software, allowing in-line changes of the device design being processed. Using inkjet printing for all layers of an OPV provides the ultimate freedom of design. This is especially beneficial for production of prototypes and up to medium scale production volumes. Also, inkjet printing requires small start-up volumes of inks and is highly economical in materials use, as there are no startup or trail ends.

[a]Holst Centre/TNO, High Tech Campus 31, 5656AE, Eindhoven, The Netherlands. E-mail: pim.groen@tno.nl
[b]Holst Centre – Solliance, High Tech Campus 21, 5656AE, Eindhoven, The Netherlands. E-mail: yulia.galagan@tno.nl
[c]Energy Research Centre of the Netherlands (ECN) – Solliance, High Tech Campus 21, 5656AE Eindhoven, The Netherlands
[d]IMEC – Solliance, Kapeldreef 75, B-3001 Leuven, Belgium
[e]Faculty of Aerospace Engineering, Delft University, Kluyverweg 1, 2629 HS Delft, The Netherlands

Inkjet printing is well known from the graphics, textile and ceramics industry, where under demanding conditions, it is reliable to run at throughput speeds far exceeding 10 m min^{-1}. The value of inkjet printing in the field of organic electronics also has been recognized. The production of high-quality conductive silver structures using inkjet printing in high-speed roll-to-roll production has been recently demonstrated for different electronic applications[19,20] as well as part of the semitransparent electrode in ITO-free OPV devices.[14] These latest developments bring roll-to-roll inkjet printing production of OPVs a step closer, by proving the feasibility of creating these devices reliably using a high-volume roll-to-roll process.

A big interest in the inkjet printing of OPV has been demonstrated over the last few years. It has been utilized for the deposition of different layers in the OPV stack. A lot of studies were focused on the inkjet printing of PEDOT:PSS[21,22] and on its use as replacement of the ITO electrode by combination with inkjet printed Ag current collecting grids.[14,23–26] Inkjet printing of OPV back electrodes has also been successfully demonstrated by different groups.[27,28] However, the main studies in last years were focused on the inkjet printing of photoactive layer.[29–32] Screening of different solvents and solvent mixture for efficient inkjet printing of P3HT/PCBM reached a very high level of interest. The best performance for an inkjet printed P3HT/PCBM blend has been reposted by Jung *et al.*[33] reaching 3.8% and was obtained by using chlorobenzene as a solvent. Recently, Jung *et al.*[34] have reported on all-inkjet-printed solar cells with power conversion efficiency of 2%. Although, results show the great potential of inkjet printing as a digital printing technology for manufacturing OPV devices, the reported approach is only suitable for few-millimeters size solar cells, because of a very high resistance of the used PEDOT:PSS electrode. Upscaling of such technology requires another printable electrode allowing large area devices. Furthermore, the most critical factor obstructing the industrial up-scaling of the approach of Jung *et al.* is the use of chlorinated solvent mixtures for the deposition of functional layers. Thus, the most challenging issues towards up-scaling all-inkjet printed solar cells remain: increasing a power conversion efficiency of large area devices, printing of large area and low resistance electrodes, printing of all layers from non-chlorinated solvents, utilizing multiple nozzles industrial printheads and demonstration of freedom of shapes and designs.

In this study, all-inkjet-printed large area (>1 cm^2) organic solar cells with power conversion efficiency of 4.1% deposited from environmentally friendly solvents are demonstrated for the first time. Moreover, organic solar cells are fabricated using industrial scale (512 nozzels) printheads, compatible with R2R technology. The reported results show that with industrial inkjet printing the switch between making different shapes of cells and modules can be done at any time during production, allowing customizable production. A large area organic solar cells with a different artistic shape also demonstrated the technique's versatility.

Experimental

Materials

Solvents were acquired from Sigma-Aldrich and used as received. High conductive poly(3,4-ethylenedioxythiophene):poly(styrenesulfonate) (HC-PEDOT, Agfa, Orgacon-IJ 1005) and PEDOT:PSS (PEDOT, Agfa, Orgacon S315) was provided by Agfa and used as received. Poly-(3-hexylthiophene) for inkjet printing (P3HT, Merck, Lisicon SP001, Mw ~ 19 kg mol^{-1}), P3HT for spin coating (Plextronics, Plexcore Mw ~ 120 kg mol^{-1}), ActivInk® PV2000 (Polyera corporation), and [6,6] phenyl C61-butyric acid methyl ester (PCBM, 99%, Solenne BV), Suntronic U5603 Ag nanoparticle ink (Sun chemicals, Slough, UK) were used as received.

Device fabrication

All device fabrication steps were performed under "clean-room 1000" conditions. The substrates for fabrication OPVs devices were either Eagle XG glass (Corning Inc., USA) or ITO covered glass substrates (sheet resistance of 10 $\Omega\ \square^{-1}$) patterned by photolithography (Naranjo, the Netherlands). Substrates were cleaned in several rinsing steps, including ultrasound treatment with Teepol industrial detergent, deionized (DI) water and isopropanol (IPA). The following stack was used as a reference: ZnO nanoparticles were synthesized according to ref. 35 using the hydrothermal condensation of Zn(acetate). After several rinsing steps, the nanoparticles were redispersed in acetone and applied by spin coating (1000 rpm, 5000 rpm s^{-1}, 60 s). The photo-active layer was spin coated either from a 2 wt%/2 wt% P3HT:PCBM solution in chlorobenzene (550 rpm, 2000 rpm s^{-1}, 95 s) or from the PV2000 ink as received from Polyera corporation (400 rpm, 5000 rpm s^{-1}, 60 s). The resulting ZnO, P3HT:PCBM and PV2000 layer thicknesses were approximately ~50, 220 and 260 nm respectively. Prior to evaporation of the back electrode, the devices were annealed at 130 °C for 10 minutes in a N_2 atmosphere for the P3HT based devices, while the PV2000 devices were annealed for 3 min at 120 °C. A MoO_x/Ag or Ag back electrode was applied by thermal evaporation with 10 + 100 or 100 nm thickness, respectively.

Ag fingers and busbars (both front and back) were inkjet printed using a Fujifilm Dimatix Materials Printer (DMP 2831). Sintering was performed either in air or in N_2 for the front and back electrode, respectively. Inkjet printing of HC PEDOT, ZnO NP, the photo-active layer and PEDOT was performed on a LP50 printing platform (Pixdro, OTB) using an industrial printhead (KM512LN, 3.5 cm width, 360 DPI nozzle spacing) and non-halogenated solvents only. ZnO nanoparticles for inkjet printing were redispersed in a veratrole–*o*-xylene mixture with concentration of 17.5 mg ml^{-1}. For the photo-active layer an ink consisting of *o*-xylene, indane and tetraline (1 : 1 : 1) was used with a 1.3 wt% concentration of both P3HT and PCBM, yielding a layer with ~240 nm thickness. On top of the inkjet printed photo-active layer a 200 nm thick PEDOT layer (Orgacon S315) was printed. The average performance of at least 5–8 devices for each type of the presented architecture was reported.

Characterization

Layer thicknesses were obtained by Dektak profilometry. Current–voltage (J–V) curves were measured using simulated solar light in a home built set-up with a halogen lamp (100 mW cm^{-2}) calibrated with a Si reference cell and using a shadow mask. Power conversion efficiencies were calculated using the short-circuit current density obtained from the EQE measurement.

Results and discussion

Semi-transparent, ITO-free, inkjet printed front and back electrodes

To obtain full freedom of design, all functional layers need to be inkjet printed, including the electrodes. Here we will first evaluate the printed electrodes in a further spin coated stack to show that these can be inkjet printed without affecting the devices performance. The first step of the study includes a replacement of ITO. The combination of conducting Ag grid lines with highly conducting PEDOT:PSS (HC-PEDOT) has been demonstrated to function as a front electrode with a sheet resistance of 7 Ω $\square^{-1}$ (ref. 24 and 25) in OPV devices with regular architecture. However, inkjet printing of this composite electrode combined with inkjet printing of a ZnO electron transport layer for manufacturing of the devices with inverted architecture has not yet been demonstrated. In this work, the Ag structures are printed using a labscale inkjet apparatus (Dimatix). However, all other layers are deposited by an industrial printhead of 3.5 cm wide, which is compatible with R2R production. While printing both the Ag and the HC-PEDOT layers on a Dimatix apparatus led to functional devices, surprisingly, devices with HC-PEDOT printed using the industrial printhead were all shunted. Closer inspection by optical microscopy revealed that coverage of the PEDOT on top of the Ag finer was inhomogeneous (Fig. 1a). Indeed, the printing direction was perpendicular to the Ag finger, and the unmerged lines of droplets are visible after drying.

The move from labscale inkjet printing equipment (with 16 printing nozzles) towards industrial printheads, allowing simultaneously use of at least 512 nozzles, requires substantial re-optimization in printing parameters, inks and substrate properties. The quality of jetting is determined by solid content, solvent composition, viscosity, surface tension and vapor pressure of an ink.[36] For the Dimatix and industrial printhead the same ink was used, and led in both cases to good droplet formation. Secondly, the surface energy and the temperature of the substrate play an important role. For both systems, the underlying substrate, a glass/Ag structure was the same. Nevertheless, with the labscale printhead the PEDOT merged to form a layer, while using the industrial printhead, the electrode remained partly uncovered. Merging of individual ejected droplets is also affected by the printhead configuration itself. For example, the drop size, which is determined by nozzle diameter, firing voltage, piezo waveform, *etc.*, was 10 μL for the labscale printhead and ~35 μL for the industrial printhead. Then, using the lab scale Dimatix printer droplets are deposited

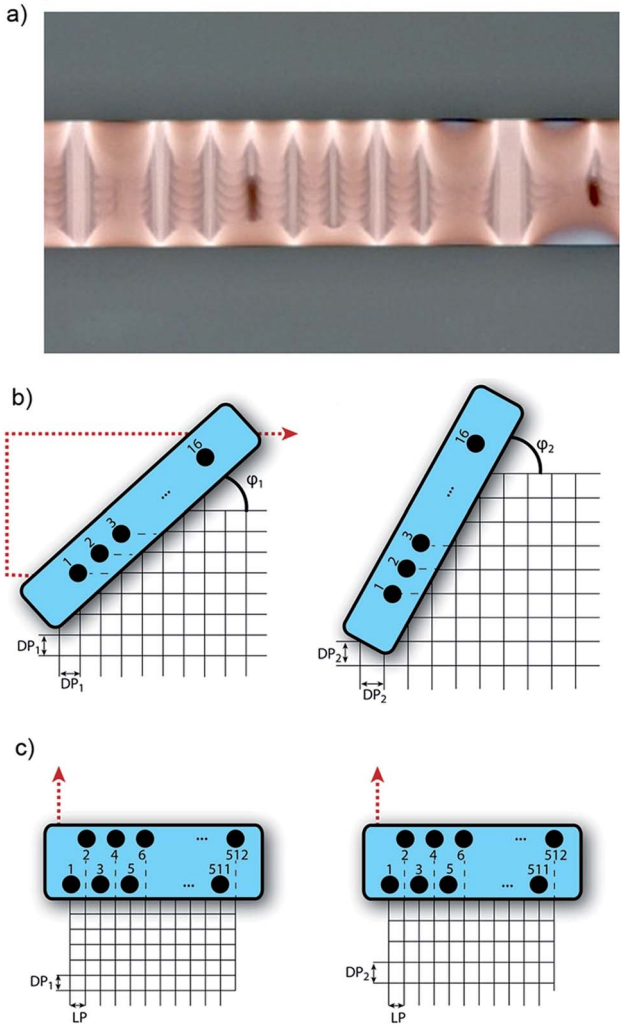

Fig. 1 (a) Optical microscopy image showing inhomogeneous coverage of HC-PEDOT printed on top of a Ag finger, (b) printing mechanism with Dimatix printheads, (c) printing mechanism with industrial printheads (arrows shows a printing direction).

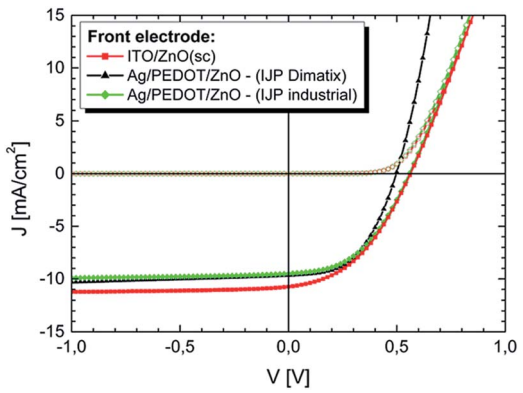

Fig. 2 J–V curves recorded for devices with a spin coated P3HT:PCBM photo-active layer and an ITO front electrode or an inkjet printed electrode consisting of IJP Ag/IJP HC PEDOT/IJP ZnO (the active area of the devices is 0.038 cm^2).

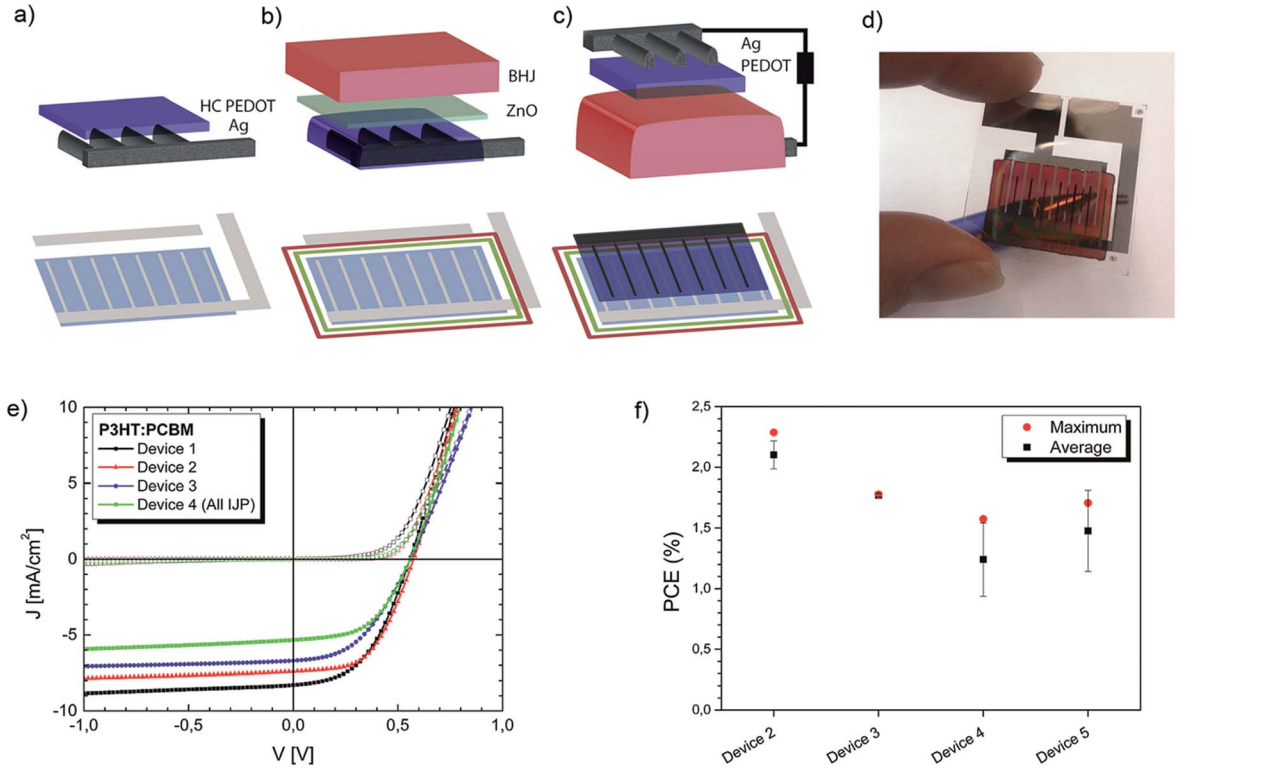

Fig. 3 (a–c) schematic representation of the layers in a fully inkjet printed organic solar cell, (d) photograph of semitransparent all inkjet printed cell, by an illumination mask a 1 cm^2 active area is defined, (e) *J–V* curves of cells with a P3HT:PCBM photo-active layer and multiple printed layers (f) maximum and average performances (back electrode is: * – Ag grids, ** – full area Ag).

in a square grid by rotating the printhead and modifying movement speed and jetting frequency (Fig. 1b). The spacing of the dot pitch (DP) of this square grid determines the amount of deposited ink per surface area and thereby layer thickness. As the grid is square, adjacent droplets are at the same distance in both directions. In case of the 512 nozzles industrial printhead used in this experiment, the printhead is always positioned perpendicular to the printing direction as rotating it would lead to loss of registry between the nozzles that are spaced in its two separate rows (Fig. 1c). The distance between adjacent nozzles therefore fixes the line pitch (LP) and layer thickness is controlled by varying the spacing of deposited droplets, dot pitch (DP), in the printing direction. This can lead to deposition of the droplets in a rectangular rather than a square pattern,

Table 1 *J–V* characteristics of cells with multiple inkjet printed layers (active area of the devices 1–5 and 8–11 is > 1 cm^2, schematic illustration of the devices is presented in Fig. 3; devices 6 and 7 have active area of 0.038 cm^2)

No.	Front contact	ETL	BHJ	HTL	Back contact	V_{oc} (V)	J_{sc} (mA cm^{-2})	FF (%)	PCE (%)
P3HT:$PC_{60}BM$									
1	ITO	SC	SC	Evap[a]	Evap	0.56	8.27	47.6	2.2
2	ITO	SC	IJP	IJP[b]	Evap	0.58	7.33	52.7	2.2
3	ITO	SC	IJP	IJP	IJP (grid)	0.56	7.05	47.5	1.9
4	IJP[c]	IJP	IJP	IJP	IJP (grid)	0.56	5.46	51.6	1.6
5	IJP	IJP	IJP	IJP	IJP (full area)	0.57	5.64	52.4	1.7
ActivInk PV2000									
6	ITO (0.038 cm^2)	SC	SC	Evap	Evap	0.75	13.3	63.5	6.3
7	ITO (0.038 cm^2)	IJP	IJP	Evap	Evap	0.78	13.4	66.9	7.0
8	ITO	SC	SC	Evap	Evap	0.76	13.4	42.0	4.3
9	ITO	SC	IJP	IJP	Evap	0.79	13.8	45.0	4.9
10	IJP	IJP	IJP	IJP	Evap	0.78	12.4	48.9	4.7
11	IJP	IJP	IJP	IJP	IJP (grid)	0.77	10.4	51.0	4.1

[a] Evaporated MoO_x. [b] IJP PEDOT. [c] IJP Ag/IJP HC PEDOT.

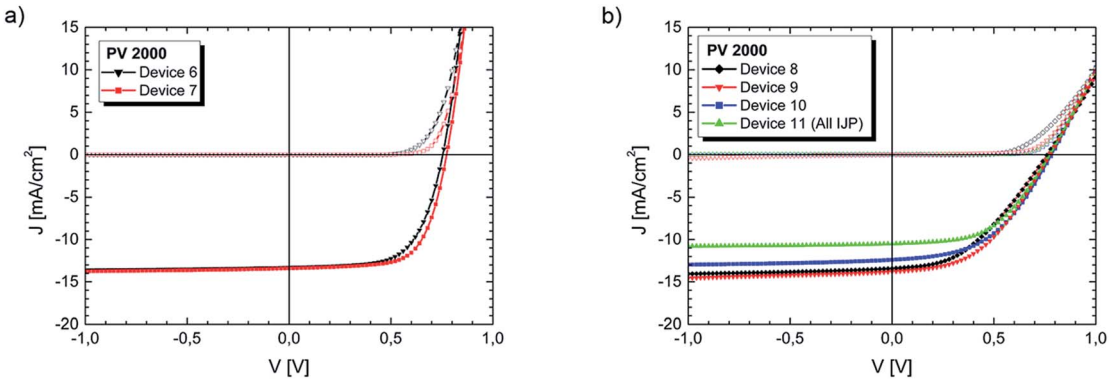

Fig. 4 J–V curves recorded for inverted OPV cells with inkjet printed PV2000 photo-active layers and (a) 0.038 cm^2 active area and evaporated back electrode, and (b) 1 cm^2 active area and up to 6 inkjet printed layers.

which can substantially influence layer formation. Thus, printing of an identical PEDOT formulation with the Dimatix and the industrial printhead ended up with different results. Tuning the dot pitch with Dimatix printer provided good merging of the droplets and a uniform closed layer could be obtained while inkjet printing with the industrial printhead did not lead to merging of the droplet lines as shown in Fig. 1a. Devices made with such low quality PEDOT layer did not show any performance. In this case either changing of printing parameters (*e.g.* substrate temperature, dot pitch, multiple printing, *etc.*) or optimization of the PEDOT formulation is required. To obtain a fully closed PEDOT layer on top of the Ag, its wetting was improved by reducing the surface tension by adding 15 wt% 2-butanol resulting in a drop in surface tension from 35.6 mN m^{-1} to 24.0 mN m^{-1} for the adjusted formulation. Although this decreased the shelf lifetime of the PEDOT, during the typical processing time span of several hours no gelation occurred. In future industrial processes the addition of 2-butanol to the PEDOT:PSS dispersion can be done in-line to prevent any lifetime issues. Using the industrial printhead Ag/HC PEDOT was printed as well as ZnO layer. The J–V curves of the devices with printed front electrodes are shown in Fig. 2. The device with the Ag/PEDOT/ZnO front electrode printed using the Dimatix platform showed as good a performance (2.3%) as compared to a cell with an ITO electrode (2.4%). A similar performance (2.3%) was obtained with the industrial printhead, using our modified formulation of PEDOT (Fig. 2). For the devices with Dimatix printed electrode the V_{oc} showed a small loss, to non-uniformity of ZnO layer. For both devices with printed Ag/PEDOT/ZnO electrode a loss in J_{sc} of ~5% compare to ITO-base device was detected, mostly due to a difference in light transmittance caused by the opaque silver grid. Relatively low FF in ITO based devices can be explained by extra resistance at ITO–ZnO interface. ZnO layer in ITO-based devices was spin coated from veratrole–*o*-xylene solvent mixture, which is adapted for inkjet printing on top of PEDOT:PSS layer.

Now the inkjet printing of the front electrodes using the industrial scale printer has been demonstrated, we focus our attention to the printing of the back electrodes. Back electrodes using solution processing of PEDOT and Ag have also been demonstrated earlier using either inkjet printing or screen printing to deposit the Ag.[28] It was shown that the usage of special type of PEDOT (Orgacon S315) prevents penetration of the solvents from the Ag inks[27,28,37] and enables manufacturing of OPV devices with inkjet printed back electrode (both full area and grids). The power conversion efficiency of such devices is

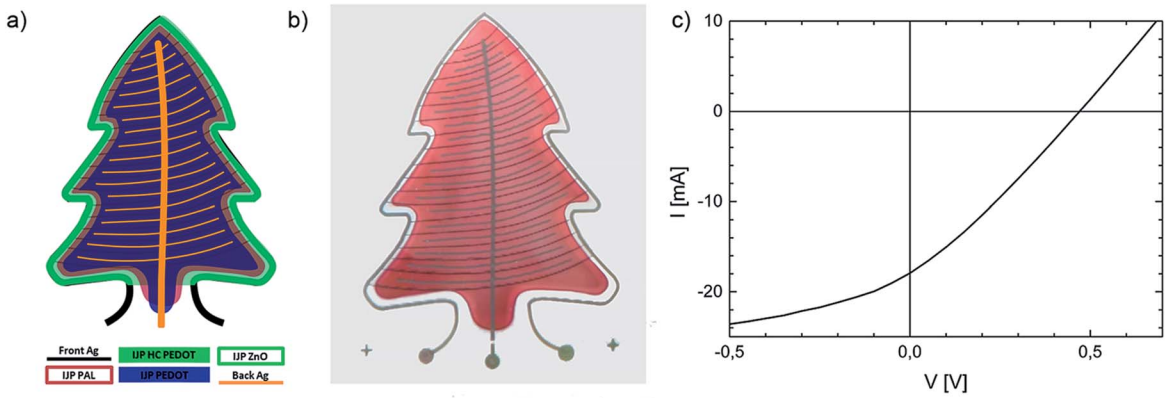

Fig. 5 Organic solar cell in the shape of a Christmas tree, (a) schematic representation of printed layers lay-out, (b) photograph of finished fully inkjet printed OPV Christmas tree, and (c) I–V curve recorded for a single device with Christmas tree shape.

comparable with the efficiency of devices with evaporated electrodes, with only a small drop in J_{sc} due to the decreased reflectivity of the printed back electrode. Sintering the Ag electrode in air also contributed to a small drop in J_{sc}, but this could be avoided by performing the sintering procedure in a N_2 environment. The average efficiency drop, observed in the devices with inkjet printed back electrodes compared to the devices with evaporated ones, is only 10–15% (ref. 28) with a yield of more than 95%. It ensures a reliable technology for the inkjet printing of back electrodes which can be implemented in all-inkjet printed devices.

Fully inkjet printed organic solar cells

Thus far, the inkjet printing of both the front and back electrodes led to a minimal loss in performance, when combined with a photo-active layer spin coated from chlorobenzene. Working towards a R2R compatible process, the use of halogenated solvents needs to be avoided. Here we inkjet print the P3HT:PCBM layer from a mixture of solvents, that yields a homogeneous layer with performance as good as the spin-coated layer.[38] As can be seen from Fig. 3e and the first two entries in Table 1, cells with an inkjet printed P3HT:PCBM layer and active area of 1 cm^2 show a small loss in J_{sc}, which is compensated by a higher FF. This layer can now be combined with the printed front electrode consisting of inkjet printed Ag, HC-PEDOT and ZnO and the back electrode consisting of PEDOT and Ag to form an all inkjet printed cell. Fig. 3a–c shows the print layout of the different layers. Careful design ensures coverage of the bottom electrode to avoid shunting between the contacts. As materials are only deposited where they are needed, no post-structuring by for instance laser scribing or wiping is required.

The performances of the fully inkjet printed cells are listed in Table 1. For a cell with a full area printed Ag back electrode a power conversion efficiency of 1.7% was achieved. For a semi-transparent cell with grids as back electrode a performance of 1.6% was measured, with a slightly lower J_{sc} due to lower light reflection. Compared to a cell with spin coated layers from halogenated solvents and ITO and evaporated metal as electrodes this corresponds to a loss of ~23% in the PCE. As can be seen in Fig. 3f, on average this loss can be attributed to the printed top electrode, even though on small area cells no loss in performance was observed (*vide supra*). Compared to an evaporated MoO_x/Ag electrode losses are expected due to light absorption in the printed PEDOT layer, less light reflectance of the inkjet printed Ag as compared to the evaporated metal as well as to the additional annealing steps. In this stack six layers are inkjet printed of which the materials from the front and back electrode are similar. Therefore, potentially by using four ink types and industrial printheads the full stack can be processed. The most important is that all layers can be inkjet printed providing the maximum degree of design freedom.

High efficiency fully inkjet printed solar cells

P3HT is still the workhorse material for many researchers in organic photovoltaics, due to its availability and price. Even though inkjet printing is done with relatively small quantities of ink, optimizing a process requires more material than a lab-scale synthesis provides, and therefore using P3HT is a logical material choice for such extensive optimization studies. To show that inkjet printing can also be applied for high efficiency materials, we here use the ActivInk® PV2000 (Polyera corporation), which has been certified at 9.1% power conversion efficiency.[39] The ink was jetted successfully from the industrial printhead and closed layers were obtained on top of the ZnO nanoparticle ETL layer. Slightly lower efficiencies were obtained in combination with this ETL (see Table 1) for both spin coated and inkjet printed PV2000 layer. Nevertheless, in a device where both the ZnO ETL and the PV2000 layer were inkjet printed a PCE of 7.0% was obtained (see Fig. 4).

The PV2000 photo-active layer yielded 4.1% efficiency in an all, *i.e.* six layer, inkjet printed cell stack. On this large area and this high current density, the sheet resistance of the electrodes influences the device efficiency more significantly. Indeed, the cell with spin-coated layers on the large area cell design showed a loss in fill factor from 65% on 0.038 cm^2 illuminated area to 42% on 1 cm^2 illuminated area. Therefore, the large area cell with a spin coated PV2000 layer, as well as with the inkjet printed PV2000 layer showed an efficiency drop to 4.2% and 4.9% respectively. The printed top electrode caused most of the efficiency loss for both the cells with the P3HT and the PV2000 material. As such, the loss in J_{sc} from 13.8 mA cm^{-2} to 10.4 mA cm^{-2} is attributed to the additional thermal treatments applied for the processing of the top electrode, in particular the sintering of the printed Ag. On the other hand, printing the front electrode led to an increase in the fill factor of the all inkjet printed cells in comparison to the ITO based cells, leading to a minimal overall loss in performance by the printing process. This experiment shows that to successfully upscale high efficiency organic photovoltaics, materials are needed that are preferably resistant towards thermal treatments and exposure to air. On the other hand, technology such as photonic sintering or UV curing of Ag back electrodes may also be applied to avoid extensive thermal treatments and most equipment can be enclosed to sustain an inert atmosphere.

Organic solar cells with freedom of design

A standardized rectangular design of the solar cells was used in the previous paragraph to demonstrate the effect of inkjet printing on device performance. Such type of design yielded a well-defined active area allowing for more straightforward comparisons. Full freedom of shape and designs is also a benefit of the inkjet printing technique. To prove this statement we here include an example of the free form design by printing the Christmas tree shown in Fig. 5. This design was not fully optimized for performance, and therefore losses are expected due to *e.g.* limited conductivity of the narrow busbars, or non-optimal length of the fingers and busbars.[24] Nevertheless, it demonstrates the capability of the inkjet printing technology presented in this paper. In the organic solar cell with a Christmas tree design the HC-PEDOT layer and ZnO ETL are printed to overlap fully with the front Ag electrode (indicated in

green, Fig. 5a). In this design, the photo-active layer falls within the ETL area, to ensure good contact line pinning. A small extension of ZnO and the PAL is printed at the stem of the tree, to provide electrical isolation between the front and back PEDOT layers. Finally, the active area is determined by the overlap area of the front electrode and back PEDOT layers, which was 6.24 cm^2. Fig. 5b shows a photograph of the printed Christmas tree, while Fig. 5c shows the IV curve recorded under illumination. Using a P3HT:PCBM photo-active layer, a V_{oc} of 0.46 V was obtained, while the fill factor was low at 28.2%. The latter is likely due to the non-optimal design. Nevertheless, this demonstrates the advantage of the freedom of design, as different sizes and shapes can be easily produced in a single experiment.

Conclusion

The freedom of design offered by inkjet printing for roll-to-roll processing of organic solar cells make it a suitable technique at the starting up phase of industrial scale production. We here show for the first time that all six layers of an inverted OPV stack can be deposited by inkjet printing under ambient conditions and while maintaining high cell performance. Inkjet printed front and back electrodes consist of Ag grid structures and a (highly) conducting PEDOT:PSS layer. After optimization both electrodes show performance equal to their lab scale equivalents, *i.e.* ITO or evaporated MoO_3/Ag. All large area thin films are deposited using an industrial scale printhead from non-halogenated solvents only. Cells with six inkjet printed layers based on P3HT:PCBM show a maximum PCE of 1.7%. This corresponds to a 23% loss in efficiency as compared to a fully spin-coated cell with ITO and an evaporated back electrode. Losses are mainly due to the top electrode and the increase in number of processing steps under ambient conditions. With the high-efficiency ActivInk PV2000 an all inkjet printed cell with 4.1% efficiency was created, showing that a switch in materials is easily made using this process. Flexibility in the choice of materials and the shape and size of cells and modules provide the necessary ability to adapt and grow with a developing market. Inkjet printing has proven its worth to the graphics, textile and ceramics industry and here demonstrates its high potential for organic electronics. It offers a route to industrialization, allowing customizable production at high volumes.

Acknowledgements

We thank the European Community's Seventh Framework Programme (FP72007-2013) under Grant no. 287818 of the X10D Project for providing financial support.

References

1 T. R. Andersen, H. F. Dam, M. Hosel, M. Helgesen, J. E. Carle, T. T. Larsen-Olsen, S. A. Gevorgyan, J. W. Andreasen, J. Adams, N. Li, F. Machui, G. D. Spyropoulos, T. Ameri, N. Lemaitre, M. Legros, A. Scheel, D. Gaiser, K. Kreul, S. Berny, O. R. Lozman, S. Nordman, M. Valimaki, M. Vilkman, R. R. Sondergaard, M. Jorgensen, C. J. Brabec and F. C. Krebs, *Energy Environ. Sci.*, 2014, **7**, 2925–2933.
2 http://www.heliatek.com/newscenter/latest_news/neuer-weltrekord-fur-organische-solarzellen-heliatek-behauptet-sich-mit-12-zelleffizienz-als-technologiefuhrer/?lang=en.
3 C.-C. Chen, W.-H. Chang, K. Yoshimura, K. Ohya, J. You, J. Gao, Z. Hong and Y. Yang, *Adv. Mater.*, 2014, **26**, 5670–5677.
4 N. Espinosa, M. Hosel, D. Angmo and F. C. Krebs, *Energy Environ. Sci.*, 2012, **5**, 5117–5132.
5 D. Kaduwal, H.-F. Schleiermacher, J. Schulz-Gericke, T. Kroyer, B. Zimmermann and U. Würfel, *Sol. Energy Mater. Sol. Cells*, 2014, **124**, 92–97.
6 P. Kopola, T. Aernouts, R. Sliz, S. Guillerez, M. Ylikunnari, D. Cheyns, M. Välimäki, M. Tuomikoski, J. Hast, G. Jabbour, R. Myllylä and A. Maaninen, *Sol. Energy Mater. Sol. Cells*, 2011, **95**, 1344–1347.
7 R. R. Søndergaard, M. Hösel and F. C. Krebs, *J. Polym. Sci., Part B: Polym. Phys.*, 2013, **51**, 16–34.
8 R. Søndergaard, M. Hösel, D. Angmo, T. T. Larsen-Olsen and F. C. Krebs, *Mater. Today*, 2012, **15**, 36–49.
9 D. Angmo, H. F. Dam, T. R. Andersen, N. K. Zawacka, M. V. Madsen, J. Stubager, F. Livi, R. Gupta, M. Helgesen, J. E. Carlé, T. T. Larsen-Olsen, G. U. Kulkarni, E. Bundgaard and F. C. Krebs, *Energy Technol.*, 2014, **2**, 651–659.
10 J. S. Yu, I. Kim, J. S. Kim, J. Jo, T. T. Larsen-Olsen, R. R. Søndergaard, M. Hösel, D. Angmo, M. Jørgensen and F. C. Krebs, *Nanoscale*, 2012, **4**, 6032–6040.
11 D. Angmo, S. A. Gevorgyan, T. T. Larsen-Olsen, R. R. Søndergaard, M. Hösel, M. Jørgensen, R. Gupta, G. U. Kulkarni and F. C. Krebs, *Org. Electron.*, 2013, **14**, 984–994.
12 G. A. dos Reis Benatto, B. Roth, M. V. Madsen, M. Hösel, R. R. Søndergaard, M. Jørgensen and F. C. Krebs, *Adv. Energy Mater.*, 2014, **3**, 1400732.
13 F. C. Krebs, J. Fyenbo, D. M. Tanenbaum, S. A. Gevorgyan, R. Andriessen, B. Van Remoortere, Y. Galagan and M. Jørgensen, *Energy Environ. Sci.*, 2011, **4**, 4116–4123.
14 D. Angmo, T. T. Larsen-Olsen, M. Jørgensen, R. R. Søndergaard and F. C. Krebs, *Adv. Energy Mater.*, 2013, **3**, 172–175.
15 F. C. Krebs, N. Espinosa, M. Hösel, R. R. Søndergaard and M. Jørgensen, *Adv. Mater.*, 2014, **26**, 29–39.
16 P. Kubis, N. Li, T. Stubhan, F. Machui, G. J. Matt, M. M. Voigt and C. J. Brabec, *Prog. Photovoltaics*, 2015, **23**, 238–246.
17 P. Kubis, L. Lucera, F. Machui, G. Spyropoulos, J. Cordero, A. Frey, J. Kaschta, M. M. Voigt, G. J. Matt, E. Zeira and C. J. Brabec, *Org. Electron.*, 2014, **15**, 2256–2263.
18 M. Singh, H. M. Haverinen, P. Dhagat and G. E. Jabbour, *Adv. Mater.*, 2010, **22**, 673–685.
19 https://www.youtube.com/watch?v=YzbENf208rA.
20 R. Abbel, P. Teunissen, E. Rubingh, T. van Lammeren, R. Cauchois, M. Everaars, J. Valeton, S. van de Geijn and P. Groen, *Transl. Mater. Res.*, 2014, **1**, 015002.

21 K. X. Steirer, J. J. Berry, M. O. Reese, M. F. A. M. van Hest, A. Miedaner, M. W. Liberatore, R. T. Collins and D. S. Ginley, *Thin Solid Films*, 2009, **517**, 2781–2786.
22 Z. Xiong and C. Liu, *Org. Electron.*, 2012, **13**, 1532–1540.
23 Y. Galagan, E. W. C. Coenen, R. Abbel, T. J. Van Lammeren, S. Sabik, M. Barink, E. R. Meinders, R. Andriessen and P. W. M. Blom, *Org. Electron.*, 2013, **14**, 38–46.
24 Y. Galagan, E. W. C. Coenen, S. Sabik, H. H. Gorter, M. Barink, S. C. Veenstra, J. M. Kroon, R. Andriessen and P. W. M. Blom, *Sol. Energy Mater. Sol. Cells*, 2012, **104**, 32–38.
25 J. J. Van Franeker, W. P. Voorthuijzen, H. Gorter, K. H. Hendriks, R. A. J. Janssen, A. Hadipour, R. Andriessen and Y. Galagan, *Sol. Energy Mater. Sol. Cells*, 2013, **117**, 267–272.
26 Y. C. Huang, F. H. Hsu, H. C. Cha, C. M. Chuang, C. S. Tsao and C. Y. Chen, *Org. Electron.*, 2013, **14**, 2809–2817.
27 D. Angmo, J. Sweelssen, R. Andriessen, Y. Galagan and F. C. Krebs, *Adv. Energy Mater.*, 2013, **3**, 1230–1237.
28 Y. Galagan, S. Shanmugam, J. P. Teunissen, T. M. Eggenhuisen, A. F. K. V. Biezemans, T. Van Gijseghem, W. A. Groen and R. Andriessen, *Sol. Energy Mater. Sol. Cells*, 2014, **130**, 163–169.
29 M. Ren, J. Sweelssen, N. Grossiord, H. Gorter, T. M. Eggenhuisen and R. Andriessen, *J. Imaging Sci. Technol.*, 2012, **56**, 040504.
30 C. N. Hoth, S. A. Choulis, P. Schilinsky and C. J. Brabec, *Adv. Mater.*, 2007, **19**, 3973–3978.
31 T. Aernouts, T. Aleksandrov, C. Girotto, J. Genoe and J. Poortmans, *Appl. Phys. Lett.*, 2008, **92**, 033306.
32 S. H. Eom, H. Park, S. H. Mujawar, S. C. Yoon, S. S. Kim, S. I. Na, S. J. Kang, D. Khim, D. Y. Kim and S. H. Lee, *Org. Electron.*, 2010, **11**, 1516–1522.
33 J. Jung, D. Kim, J. Lim, C. Lee and S. C. Yoon, *Jpn. J. Appl. Phys.*, 2010, **49**, 05EB031–005EB035.
34 S. Jung, A. Sou, K. Banger, D.-H. Ko, P. C. Y. Chow, C. R. McNeill and H. Sirringhaus, *Adv. Energy Mater.*, 2014, 1400432.
35 W. J. E. Beek, M. M. Wienk, M. Kemerink, X. Yang and R. A. J. Janssen, *J. Phys. Chem. B*, 2005, **109**, 9505–9516.
36 I. Burgues-Ceballos, M. Stella, P. Lacharmoise and E. Martinez-Ferrero, *J. Mater. Chem. A*, 2014, **2**, 17711–17722.
37 M. Hösel, R. R. Søndergaard, D. Angmo and F. C. Krebs, *Adv. Eng. Mater.*, 2013, **15**, 995–1001.
38 T. M. Eggenhuisen, Y. Galagan, E. W. C. Coenen, W. P. Voorthuijzen, M. W. L. Slaats, S. A. Kommeren, S. Shanmugam, M. J. J. Coenen, R. Andriessen and W. A. Groen, *Sol. Energy Mater. Sol. Cells*, 2015, **134**, 364–372.
39 http://www.pv-tech.org/news/polyera_claims_9.1_power_conversion_efficiency_on_its_opv_cell.

